10

Direct femtosecond laser writing of birefringent microtracks in bulk fused silica

© A.E. Rupasov, I.V. Gritsenko, N.I. Busleev, G.K. Krasin, Y.S. Gulina, A.V. Bogatskaya, S.I. Kudryashov

Lebedev Physical Institute, Russian Academy of Sciences, 119991 Moscow, Russia

e-mail: rupasovan@lebedev.ru

The characteristics of birefringent microtracks inscribed by ultrashort laser pulses with varied parameters in the volume of fused silica have been studied. In particular, the formation of birefringent microtracks with a phase shift of up to $150°$ degrees is observed, and the direction of the slow axis coincides with the direction of the linear polarization vector of the inducing laser radiation. The physical mechanisms of modification of fused silica using Raman scattering have been revealed. Using a spectrophotometer microscope, transmission and reflection spectra of birefringent regions consisting of microtracks were obtained.

Keywords: birefringence, micromodification, fused silica, direct laser writing, ultrashort laser pulses.

DOI: 10.61011/EOS.2024.01.58296.12-24

1. Introduction

In recent years, laser writing of microtracks induced by ultrashort pulses in bulk of transparent solid dielectrics has been actively developing. A special feature of these microtracks is the birefringence effect [1]. Birefringent microtracks are permanent material modifications formed along the axis of radiation propagation. Birefringence herein is caused by the presence of an ordered submicron substructure [2] with a period less than the wavelength of the inducing laser radiation, which represents the areas of compaction and decompression of the material [3]. To date, a number of mechanisms have been proposed that explain the formation of the microtrack substructure, for example, incident emission interference [4], plasmon interference [5,6] and exciton-polariton interference [7].

Based on the laser recording of birefringent microstructures, technologies such as optical memory [8,9] and fabrication of phase optical elements [10–12] are actively developing today.

This study has investigated whether uniform birefringent regions based on microtracks in bulk of fused silica can be recorded with tight focusing of laser radiation. Structural changes in the recorded region have been investigated using Raman scattering.

2. Experimental setups

Fused silica is now the main material for in bulk recording birefringent microtracks that are widely used for development of optical phase elements and optical memory [9,10]. In this study fused silica KU-1 („Elektrosteklo") was used that is transparent in the range from 170 nm to 2600 nm.

The sample was 3 mm thick with all its facets preliminary polished.

Satsuma ytterbium fiber laser with a fundamental wavelength of 1030 nm was used as a source of laser pulses. Pulse duration varies in the range from 0.3 ps to 10 ps, pulse repetition rate varies from 1 Hz to 500 kHz, maximum pulse energy is $10 \mu J$. Radiation was focused in bulk of fused silica using a microlens with numerical aperture $NA = 0.45$ (Figure 1).

Series of tracks with spacing $10 \mu m$ and $100 \times 2000 \mu m$ in size were recorded in bulk of the fused silica exposed by 0.3 ps and 0.6 ps pulses with pulse energies from $0.25 \mu J$ to $3.5 \mu J$ at a depth of 1 mm, with pulse repetition rate 100 kHz. The fused silica sample was moved using Prior XYZ automatic linear translator at a rate of $300 \mu m/s$. Pulse duration was measured using Avesta AA-10 DD-12 PS scanning interference autocorrelator.
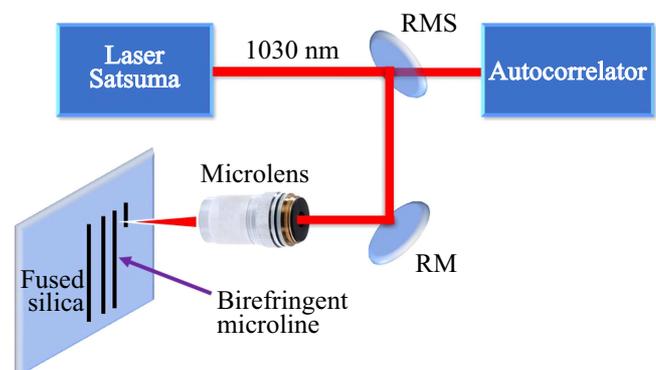
Figure 1. Experimental setup for laser writing of birefringent microstructures: RMS — folding mirror, RM — mirror.
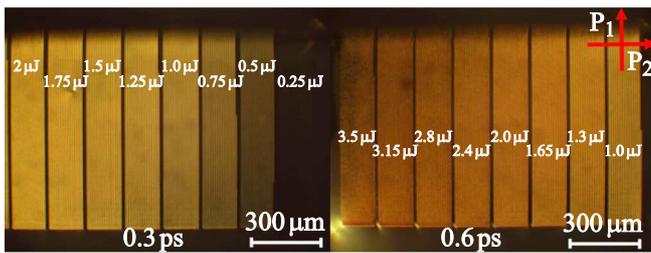
Figure 2. Optical images of the recorded areas in crossed polarizers.

Thorlabs LCC7201 system was used to investigate birefringence. This system is used to measure phase shift up to $180°$ (light source wavelength $633\,nm$) and slow axis direction within $\pm 90°$.

To study structural changes in the birefringent microtrack formation region, Confotec MR350 confocal scanning microscope was used. The photoluminescence signal was used to estimate the thicknesses of the recorded structures. Investigations were carried out using $532\,nm$ laser in $5\,\mu m$ range (lens $NA = 0.3$).

Reflection and transmittance of the birefringent microtracks were measured using LOMO MSFU-K microscope spectrophotometer. The microscope allows you to measure the reflectance and transmittance spectra in the micron-range. Halogen lamps were used as light sources.

3. Experimental results and discussion

3.1. Optical investigations

Regions consisting of birefringent microtracks were recorded in bulk of the fused silica. Phase shift can be controlled by varying the laser radiation parameters. Birefringent microtracks were visualized using an optical microscope, where regions in crossed polarizers are colored in birefringent colors (Figure 2).

As shown in Figure 2, phase shift can be controlled by changing pulse energy and duration. During the study, a threshold regime for the formation of birefringent microtraces was discovered — pulse energy $0.25\,\mu J$, below which no microtracks were formed.

3.2. Polarimetric investigations

Phase shift of the recorded regions throughout the sample depth was measured using the polarimetric system (Figure 3.). Maximum phase shift of birefringent microtracks was equal to $\sim 150°$.

As shown in Figure 3, the recorded regions have good uniformity in phase shift, allowing writing millimeter areas. This will make it possible to develop phase optical elements, the dimensions of which will not be limited by technology, but only by an experimental setup.

Figure 4 demonstrates the azimuth orientation of birefringent microtracks. Slow axis (azimuth) direction demonstrates the maximum change in refraction index in the recorded regions. The direction of the slow axis of birefringent microtracks coincides with the direction of the linear polarization vector of the laser radiation inducing microtracks. Thus, the microtrack slow axis (azimuth) direction can be controlled by rotating the linear polarization vector of laser radiation.

3.3. Raman scattering

Raman scattering was investigated in the birefringent microtrack formation area. The samples were preliminary cut into halves for direct access to the structures recorded in bulk of the fused silica (Figure 5, a). The 490, 605 and $805\,cm^{-1}$ bands in the Raman scattering spectrum are responsible for Si-O-Si bridge bonds (Figure 5, b), therefore, structural modifications and fused silica transformation may be assessed by change in the relationship between amplitudes of these peaks. It should be noted separately that the photoluminescence signal grows significantly in the birefringent microtrack formation region. This growth can be associated with oxygen deficiency as a result of laser machining [13].

Relationship of peak amplitudes at 490, 605 and $805\,cm^{-1}$ in Figure. 5, b suggests that material compaction occurs in the laser modification region due to photoinduced break of Si-O-Si bridge bonds[14,15].

Thus, during laser processing, the initial material is transformed, which leads to a change in the Raman spectrum of laser-modified fused silica towards compacted fused silica.

3.4. Reflectance and transmittance of recorded regions

The reflection and transmission spectra of birefringent regions were obtained using a spectrophotometer microscope(Figure 6).

As shown in Figure 6, a, the birefringent microtrack reflectance decreases with increasing pulse energy, but the reflectance changes negligibly compared with the initial material. At the same time, as shown in Figure 6, b, transmittance of the modified regions decreases considerably with pulse energy growth that may be associated with light scattering on birefringent microtracks. For a pulse energy of $0.25\,\mu J$, transmittance of birefringent regions is comparable with transmittance of the unmodified fused silica as observed earlier [16].

4. Conclusion

The study has investigated whether uniform birefringent microtracks can be recorded by subpicosecond laser pulses with varied parameters.
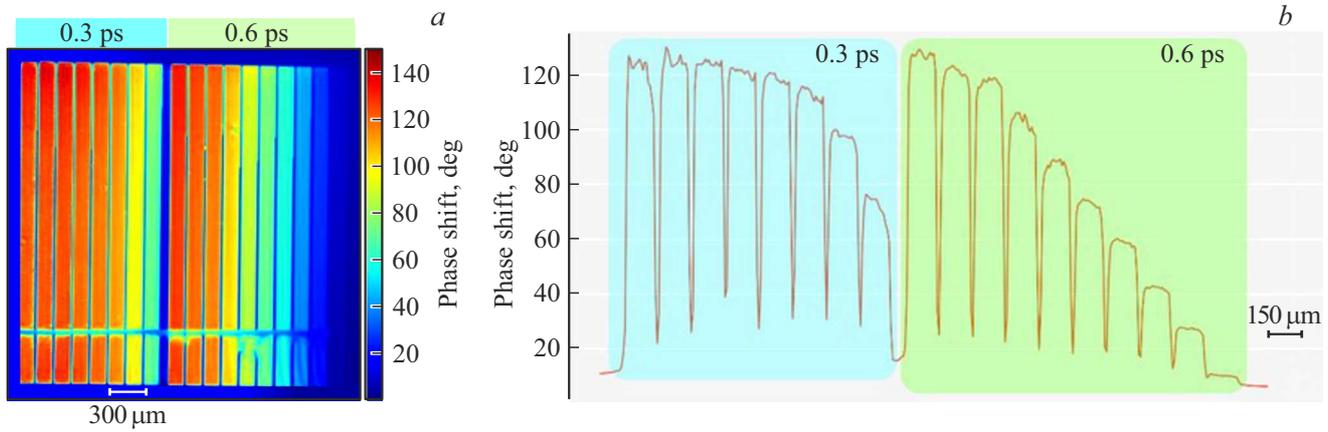
Figure 3. Polarimetric images of birefringent microtracks in bulk of the fused silica: (*a*) pseudocolor chart of phase shift values, (*b*) region profiles with phase shift values.
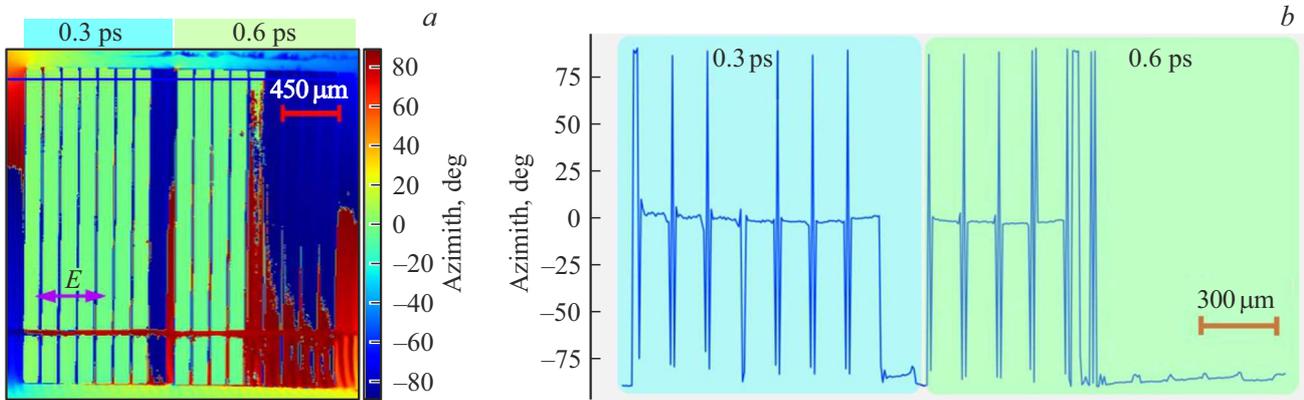
Figure 4. Polarimetric images of birefringent regions consisting of microtracks in bulk of the fused silica: (*a*) pseudocolor chart of azimuth values, (*b*) region profiles with azimuth values. *E* — shows the linear polarization vector direction that existed during laser recording.
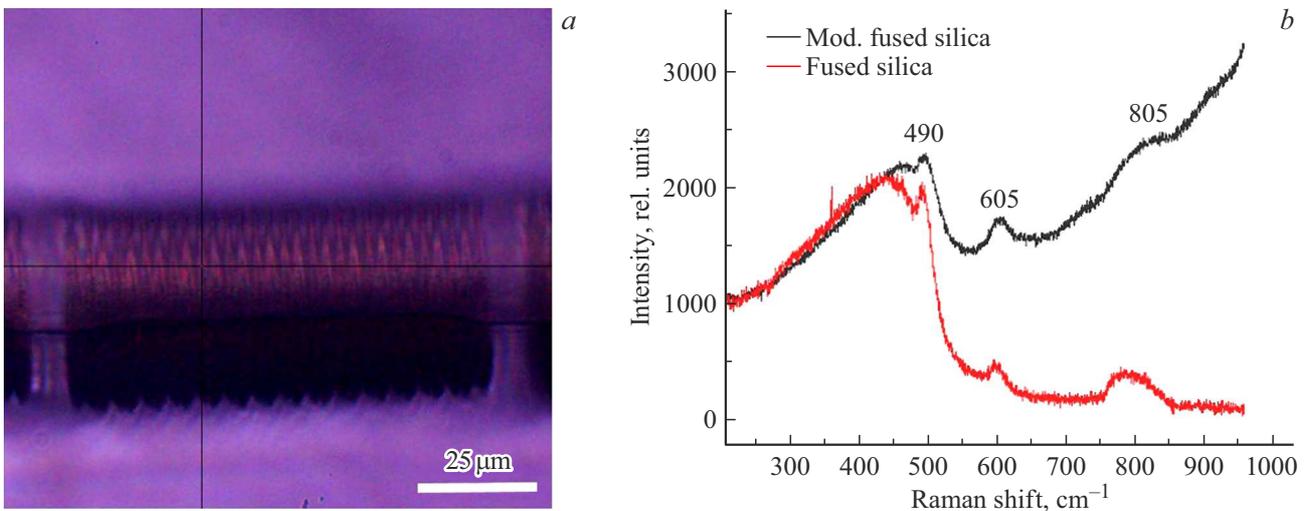
Figure 5. (*a*) The optical image of birefringent microtrack section. (*b*) Raman scattering spectra — initial spectrum of the sample (red) and modified region spectrum (black).
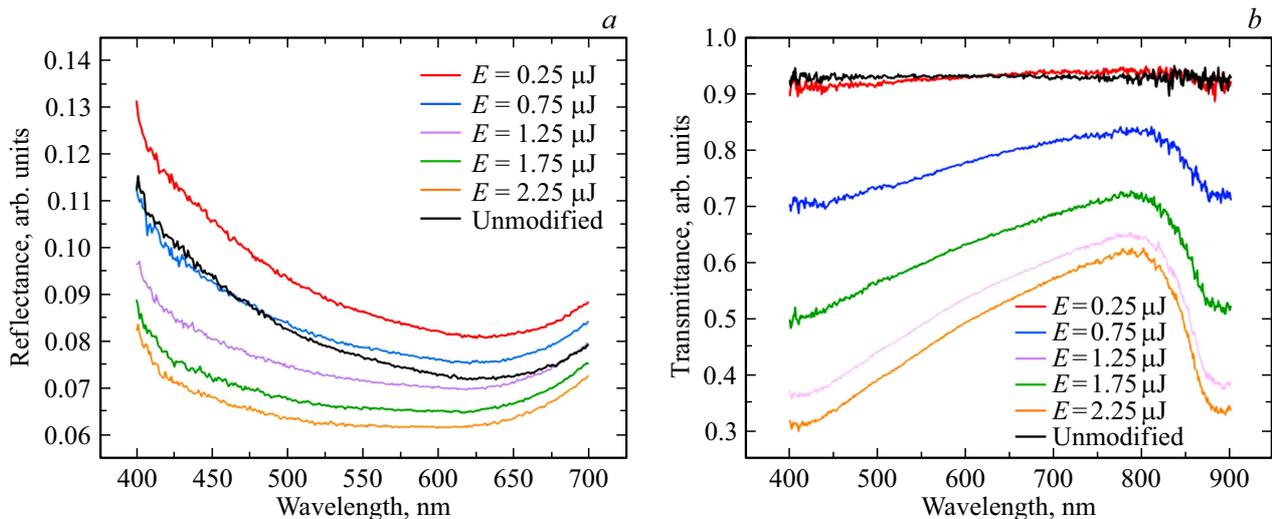
Figure 6. (*a*) Reflection spectra of the recorded regions in bulk of the fused silica and initial unmodified material. (*b*) Birefringent microtrack transmittance spectra in bulk of the fused silica and initial unmodified material.

It has been found that the maximum phase shift of birefringent regions is equal to $\sim 150°$. The direction of the slow axis of the recorded structures coincides with the direction of the linear polarization vector of the inducing laser radiation.

The Raman scattering study suggests that the fused silica is compacted in the birefringent microtrack formation region due to photoinduced break of Si−O−Si bridge bonds.

The analysis of the recorded transmittance spectra of the birefringent microtracks has shown that transmittance decreases considerably in the inscribed regions, therefore, the use of such structures for fabrication of phase optical elements and optical memory is severely limited.

Funding

Conflict of interest

The authors declare that they have no conflict of interest.

References

[1] Y. Shimotsuma, K. Hirao, J. Qiu, P.G. Kazansky. Mod. Phys. Lett. B, **19** (5), 225 (2005).

[2] R. Taylor, C. Hnatovsky, E. Simova. Laser Photonics Rev., **2** (1−2), 26 (2008).

[3] E. Bricchi, B.G. Klappauf, P.G. Kazansky. Opt. Lett., **29** (1), 119 (2004).

[4] Y. Shimotsuma, P.G. Kazansky, J. Qiu, K. Hirao. Phys. Rev. Lett., **91** (24), 247405 (2003).

[5] S. Kudryashov, A. Rupasov, M. Kosobokov, A. Akhmatkhanov, G. Krasin, P. Danilov, B. Lisjikh, A. Abramov, E. Greshnyakov, E. Kuzmin, M. Kovalev, V. Shur. Nanomaterials, **12** (23), 4303 (2022).

[6] S. Kudryashov, A. Rupasov, M. Smayev, P. Danilov, E. Kuzmin, I. Mushkarina, A. Gorevoy, A. Bogatskaya, A. Zolotko. Nanomaterials, **13** (6), 1133 (2023).

[7] M. Beresna, M. Gecevičius, P.G. Kazansky, T. Taylor, A.V. Kavokin. Appl. Phys. Lett., **101** (5), 053120 (2012).

[8] E.N. Glezer, M. Milosavljevic, L. Huang, R.J. Finlay, T.H. Her, J.P. Callan, E. Mazur. Opt. Lett., **21** (24), 2023 (1996).

[9] H. Wang, Y. Lei, L. Wang, M. Sakakura, Y. Yu, G. Shayeganrad, P.G. Kazansky. Laser Photonics Rev., **16** (4), 2100563 (2022).

[10] M. Beresna, M. Gecevičius, P.G. Kazansky, T. Gertus. Appl. Phys. Lett., **98** (20), 562 (2011).

[11] J.D. Mills, P.G. Kazansky, E. Bricchi, J.J. Baumberg. Appl. Phys. Lett., **81** (2), 196 (2002).

[12] M. Beresna, M. Gecevičius, P.G. Kazansky. Adv. Opt. Photonics, **6** (3), 293 (2014).

[13] H.B. Sun, S. Juodkazis, M. Watanabe, S. Matsuo, H. Misawa, J. Nishii. J. Phys. Chem. B, **104** (15), 3450−3455 (2000).

[14] J.W. Chan, T. Huser, S. Risbud, D.M. Krol. Opt. Lett., **26** (21), 1726 (2001).

[15] J. Burgin, C. Guillon, P. Langot, F. Vallée, B. Hehlen, M. Foret. Phys. Rev. B, **78** (18), 184203 (2008).

[16] HI. Busleev, A.E. Rupasov, V.V. Kesaev, N.A. Smirnov, S.I. Kudryashov, R.A. Zakoldaev. Opt. i spektr., **131** (2), 170 (2023). (in Russian)

Translated by E.Ilinskaya